Characterization of a Split Circle Element for Microstrip Reflectarrays

Khalil H. Sayidmarie[1] and Likaa S. Yahya[2]

[1]*Ninevah University, Mosul, Iraq,*
[2]*Northern Technical University, Mosul, Iraq*

Abstract — A split circular element is proposed as a unit cell for reflectarray antennas. The unit cell is derived from a circle divided into four equal sectors. The radius of two oppositely located sectors is then scaled by a certain factor to form the proposed shape. The CST Microwave Studio Suite software simulator was used to investigate the performance of the proposed unit cell, which was evaluated using Floquet port excitation. The designed element's reflection phase range was compared to that of a conventional circular patch. Four scenarios of varied substrate characteristics are investigated for the antenna to establish the best performance parameters. The simulations showed that a basic substrate with a thickness of 0.16 mm and a dielectric constant of 3.2, backed by a 3 mm foam with a dielectric constant of 1.05 and a scaling factor of 0.72 offers a wide phase range of 601.3°. The obtained phase slope is 76.37°/mm or 134°/GHz.

Keywords — *microstrip antenna, reflectarray antenna, split circular, X band*

1. Introduction

A microstrip reflectarray is a flat array of microstrip patches or dipoles printed on a thin dielectric substrate. A feed antenna illuminates the array, where each element is designed to scatter the incident field with the proper phase to make a planar phase surface in the presence of the aperture [1]. Reflectarrays thus combine the features of flat arrays and reflector antennas, and microstrip reflectarrays have emerged as a prospective solution that offers high gain and higher efficiency levels at a lower cost [2], [3].

Several resonant element designs using sophisticated approaches have been presented in the literature. These include double concentric rings [4], a double-cut ring with varying sizes [5], an elliptical dipole, slot lines, as well as a ground plane [6]. Dual band and dual circular polarizations were employed in the design of a reflectarray antenna for space communications in [7]. In this paper, a unit cell comprises two rings, an inner ring adjusted at the Ka band and a larger ring suited for the K band. The phase and amplitude of the reflecting field are regulated by stubs loaded with rings [7]. Patch elements with a cross loop and a square ring slot loaded patch were proposed in [8]. Many varied forms of fundamental elements [9]–[10], structures with multiple layers [11]–[13], and rotation methods [14], [15] were also presented in various research papers.

For the design of reflectarray unit cells, some fractal patch topologies with low losses, small sizes and appropriate phase ranges were proposed in [16], [17]. The self-similarity feature characterizes fractal geometries, where a specific shape is scaled and repeated several times to generate the final fractal shape. In practice, a fractal shape is created using an iterative technique that includes an initial shape, also known as the fractal generator, a scaling factor s used to shape the dimensions to be scaled, and the repetition number [18]. The fractal reflectarray antenna is a technique that is widely used in antenna design, for example [16], [17] describe variable-sized fractal reflectarray units. These investigations aim to attain a phase range greater than 360° and a lower gradient in the reflection phase graph, as a function of element size [17], [18]. The use of the fractal geometries offers a wider bandwidth, resulting from the various dimensions offered by the fractal shapes, as seen in paper [18]. To further enhance the solution's performance, a multilayer design and fractal geometry with aperture coupling were also employed in [19].

In [20], an asymmetric rectangular patch reflectarray antenna, comprising a single layer, is presented for 5G communication at 26 GHz. The idea is to produce two active lengths leading to two different frequencies, thus widening the bandwidth.

This paper aims to design a reflectarray unit cell element offering more than one resonance response on a single layer. The many resonance responses are then used to obtain an extension in the reflection phase range and lower slope. The circular patch providing smaller phase slopes [21] is utilized here to propose a split circle element that can achieve a double resonance response at a lower slope. The split circle microstrip unit element is investigated for the X band reflectarray design.

The paper is organized in the following manner. Section 2 presents the design of the proposed unit cell. The results of the investigations are presented in Section 3. The performance of the proposed unit cell is compared with that of other published elements in Section 4, while conclusions are drawn and described in Section 5.

2. Design of the Unit Cell Element

For reflectarrays, the unit cell element should provide a phase range in excess of 2π radians and should be characterized by low sensitivity to size and frequency changes. An inadequate
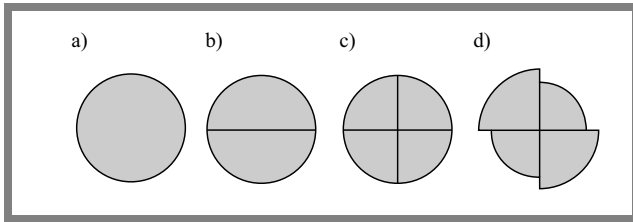
Fig. 1. Evolution of the split circle: a) circle, b) split into two sectors, c) split into four sectors and d) opposite sectors are scaled.

phase range might cause phase errors on the array, resulting in poor radiation pattern performance [21]. To extend the range of the phase response up to the full swing of 360°, a unit cell split circle is proposed here to enhance the array's performance.

The evolution of the proposed split-circle element is depicted in Fig. 1. This unit cell is derived from a circle of diameter d that is divided into two halves by the diagonal. Then, each half is further divided into two halves along the other perpendicular diagonal, resulting in four adjacent sectors. The radius ($r = \frac{d}{2}$) of two oppositely located sectors is then scaled by a certain factor, as shown in Fig. 1. The four sectors are kept in contact forming a single conducting element placed on one side of a grounded substrate. The multi-dimension features in this proposed element generate more than one resonance frequency and thus increase the bandwidth of the unit cell.

The research begins with a unit cell element designed for an X band microstrip reflectarray with a central frequency of 10 GHz. Taconic TLY-5 substrate with relative permittivity of 2.2 and loss tangent $\tan \delta$ of 0.0009 is used as a separator between the ground plane and the reflecting patch. The unit cell size is 18.1×18.1 mm, which corresponds to $0.6 \times 0.6 \lambda_o$, where λ_o is free space wavelength at an operating frequency of 10 GHz.

3. Simulation Results

The proposed unit cell was investigated using the CST Microwave Studio simulator. The frequency solver was employed to determine the unit cell's characteristics. As illustrated in Fig. 2, unit cell boundary conditions are used in the transverse x and y directions, while Floquet port boundary conditions are used in the positive z direction. The incident wave is assumed to propagate in the negative z direction.

3.1. Phase Range Performance

The simulations comprised four cases. In case 1, the element is mounted on top of a 3.175 mm thick Taconic TLY-5 substrate ($\varepsilon_r = 2.2$ and $\tan \delta = 0.0009$) which is backed by a conducting ground plane with a thickness of 0.035 mm. Case 2 uses identical properties, except for the fact that the thickness of the substrate is altered to 1.57 mm. In the third scenario (case 3), ε_r is set to 3.2, while the remaining substrate parameters remain unchanged. In case 4, the active element is printed on a 0.16 mm thick Taconic TLY-5 substrate supported by a 3 mm thick foam layer with $\varepsilon_r = 1.05$.
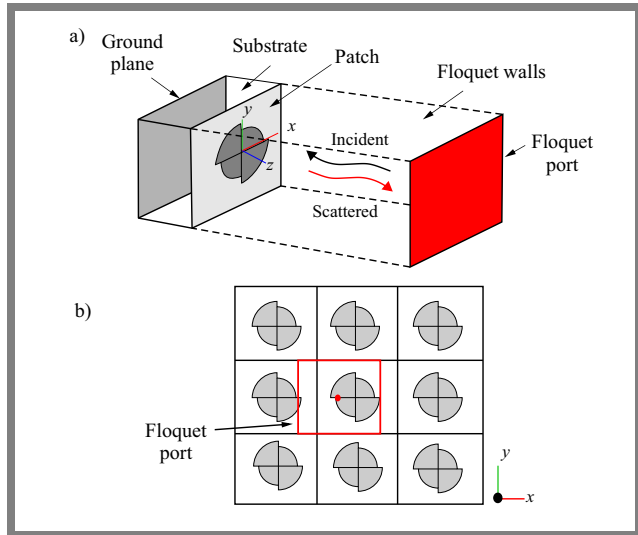

Fig. 2. The Floquet technique: a) boundary conditions of a unit cell and b) CST MWS model of an infinite periodic array.
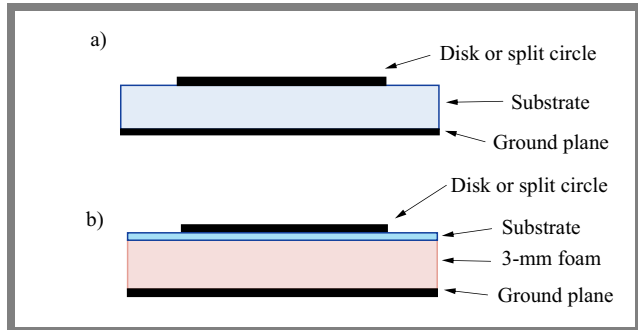

Fig. 3. Details of the antenna substrate configurations for: a) cases 1–3 and b) case 4.
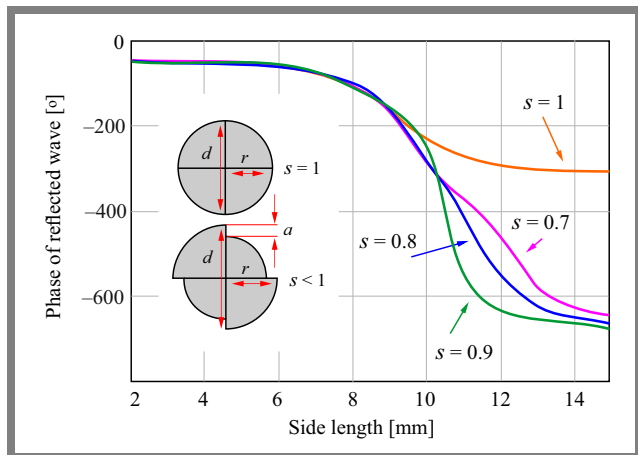

Fig. 4. Case 1 phase responses of the disk and split circle structures.

Figure 3 shows the antenna substrate configurations for all four cases. The phase responses for a unit cell including the disk or split circular patch on a single-layer substrate are given in each case. Outer diameter d determines the phase and magnitude of the reflected wave. Scale factor s is given for four alternative values in each scenario (1, 0.9, 0.8, 0.7). Figures 4, 5, 6, and 7 demonstrate the phases of a unit cell's reflected wave as a function of its diameter. The results were
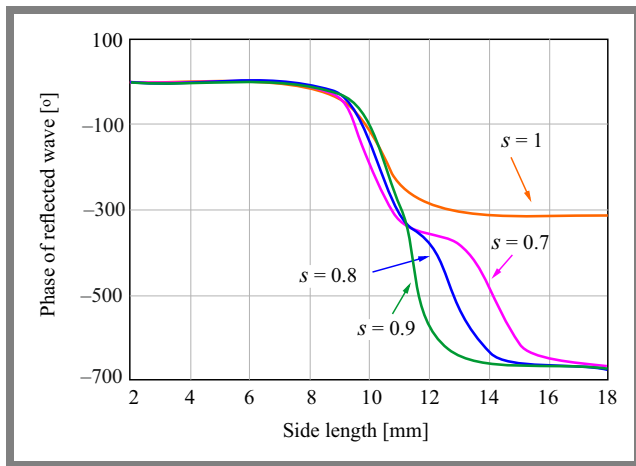
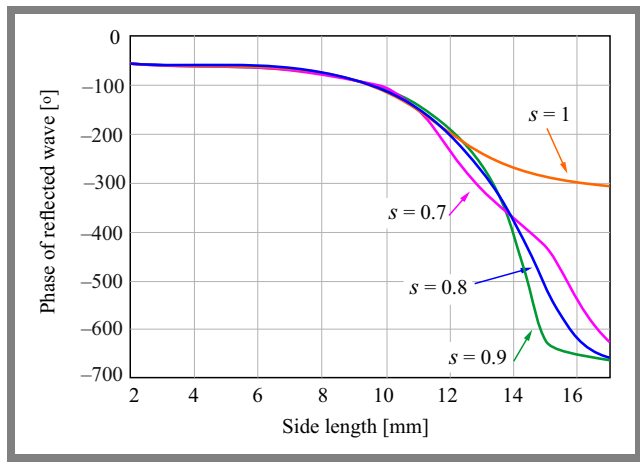**Fig. 5.** Case 2 phase responses of the disk and split circle structures.

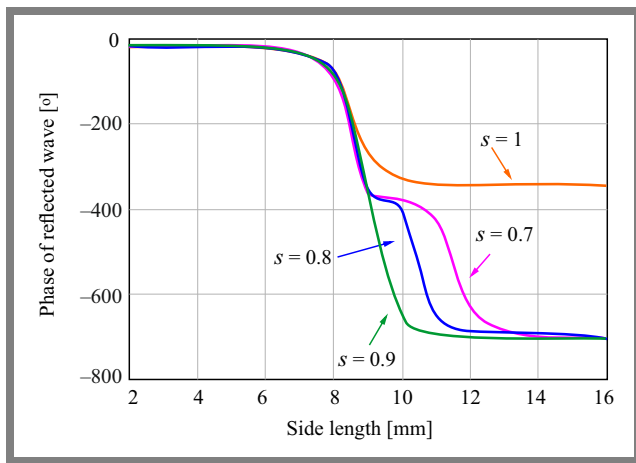**Fig. 6.** Phase responses of the disk and split circle in case 3.

Fig. 7. Phase responses of the disk and split circle in case 4.

Fig. 8. Reflection coefficient features for the four simulated cases: a) magnitude responses versus frequency, b) phase responses versus frequency, and c) phase responses with diameter d.

arranged in four cases, as described below. Figure 4 shows the simulation results for case 1. One can see that the disk element ($s = 1$) has a phase range of 257.2°, which is less than the required value of 360°. This result is congruent with the finding presented in [21]. By decreasing s from 0.9 to 0.7 (split circle), the phase range is expanded to approx. 615° by altering d from 2 to 15 mm. It is also demonstrated that with the growing the value of s, the phase gradient decreases.

For case 2, the results are displayed in Fig. 5. The phase range was greater than in the previous case, and reached approx. 663°. As s was decreased from 0.9 to 0.7, the slope becomes less linear than in case 1, particularly at $s = 0.7$.

Figure 6 depicts the results for case 3. The obtained phase range is 686°, which is better than in the two previous cases. However, the linearity of the phase response deteriorates with the growing s parameter.

Figure 7 depicts the effect of attaching a 3 mm foam substrate with a dielectric constant of 1.05 to the element with a thickness of 0.16 mm and a dielectric constant of 3.2 (case 4). While lowering the s parameter from 0.9 to 0.7, the linearity remains good as compared with cases 2–3, while the phase range is 592°, which is less than in the preceding simulations. The value is sufficient, however, to develop a reflectarray antenna.

3.2. Reflection Loss and Phase Slope of Reflection

The amplitude and phase responses of the reflection coefficients that were obtained as best values of the four cases are shown in Fig. 8. The results were gathered for $d =$10.8, 11.0, 9.0, and 12.7 mm for the four cases, respectively. As seen in

Fig. 8a, the presence of a split circle results in two resonances in the magnitude of s parameters. The resonances are caused by the unit cell's small and large sectors, and the reflection amplitude varies between –2.9 dB in case 3 to –0.12 dB in case 4. It is worth noting that when the magnitude of the reflection coefficient approaches zero, then the reflection tends to be perfect or the unit cell is experiencing smaller losses. To assess the phase range performance of different reflection phase curves, a figure of merit (FoM) related to the slope of the phase curves has been created. The FoM is provided by [2]:

$$FOM = \frac{\Delta\theta}{\Delta f} , \qquad (1)$$

or a phase slope that can be expressed by [17]:

$$Phase\ slope = \frac{\Delta\theta}{\Delta L} , \qquad (2)$$

where $\frac{\Delta\theta}{\Delta f}$ signifies the phase variation with the frequency determined at the phase center and $\frac{\Delta\theta}{\Delta L}$ denotes the change in the reflection phase with size calculated at the phase center. Therefore, FoM is calculated in degrees per GHz and phase sensitivity is computed in degrees per millimeter. To improve bandwidth performance, the FoM, or slope of the phase curve around the resonance of a reflectarray antenna, must be as low as possible [17], [21]. Figures 8b and 8c illustrate the simulated reflection phases versus frequency and size for the best values of four cases. The thicker substrate (case 1 and case 4) produces a linear phase and slow fluctuation as compared to cases 2–3, as indicated by the phase responses presented in Figs. 8b and 8c and the computed values of their properties provided in Tab. 1. The smallest slopes in terms of size and frequency are obtained in case 4, which is equal to 76.37° per mm and 134° per GHz with a phase range of 601.3°. It is also noted that case 4, with a minimum FoM value of 134° per GHz, has the minimum phase range of approx. 601.3°, but case 3, with a maximum FoM of 263.1° per GHz, has a maximum phase range of 678.6°. It is clear that the phase range is related to the FoM.

In order to calculate the element's bandwidth from phase fluctuation, a maximum limit of 180° for the change in phase when the frequency varied is considered. With such a limit, an oscillating phase swing of $\pm 90°$ from the value at the center frequency of operation is thought to be sufficient to degrade the array's radiation pattern. Such a phase change limit was taken into account when estimating the reflectarray bandwidth in [22]. Table 2 lists the calculated bandwidths from the responses displayed in Fig. 8b. When compared to the other cases, the element in case 1 has a 13.4% wider bandwidth.

4. Comparison to Existing Papers

The performance of the proposed unit cell element is compared to earlier works utilizing various element structures. Table 3 summarizes the comparative performance of unit cell reflectarray antennas. The table shows that the developed design delivers a phase variation of 601.3° throughout a frequency range in the X band (8–12 GHz), which is greater than

Tab. 1. Calculated phase response properties, and substrate details for the split circle unit cells, as depicted in Figs. 8b and 8c.

Parameter	Case 1	Case 2	Case 3	Case 4
Gradient [°/mm]	83.48	161	196	76.37
Gradient [°/GHz]	137.8	241.0	263.1	134
Max. phase [°]	–48.9	3.12	–18.57	–57.29
Min. phase [°]	–645.2	–670.6	–697.2	–658.6
Phase range [°]	596.3	673.7	678.6	601.3
ε_{r1}	2.2	2.2	3.2	3.2
Substrate thickness h_1 [mm]	3.175	1.57	1.57	0.16
ε_{r2} (foam)	–	-	-	1.05
Foam thickness h_2 [mm]	–	-	-	3

Tab. 2. Calculated bandwidths for the split circle unit cells depicted in Fig. 8b.

	θ at f_r [°]	f_1 at $\theta-90^o$ [GHz]	f_2 at $\theta+90^o$ [GHz]	BW f_2-f_1	Percent BW
Case 1 s=0.66	–356.9	10.64	9.30	1.34	13.4
Case 2 s=0.85	–143.6	10.23	9.61	0.62	6.2
Case 3 s=0.85	–326.5	10.60	9.68	0.92	9.2
Case 4 s=0.72	–289.9	10.60	9.40	1.20	12

the phase range achieved in the majority of the remaining papers. Nevertheless, the element size is larger when compared with the majority of other references. The area of the unit cells ranged from 0.43×0.43 to 0.94×0.94 effective wavelengths, with the proposed unit cell within the range. The smooth phase curve of the suggested unit cell yields a lower maximum phase sensitivity of 76.37° per mm when compared to the values presented in [9], [13] and [26].

5. Conclusions

A single-layer microstrip reflectarray element has been proposed and investigated. The element's development is based on a traditional circular patch element. Using the proposed technique, two distinct resonance frequencies can be obtained from a single element. Expansion of the reflection

Tab. 3. Comparison of the performance of the proposed unit cell with earlier works.

Reference, type of element	Phase range [°]	Area [mm²] $\lambda_g \cdot \lambda_g$	Slope [°/mm]	Resonance freq. [GHz]	Substrate type	ε_{r1}	Substrate thickness [mm]	Air, foam or second layer [mm]	tg δ
[4], single layer two concentric rings	450	15 × 15 (0.43×0.43)	NA	11.5	NA	2.2	0.508	6.35 foam	0.0009
[5], single layer double cut ring	≅ 300	12.5 × 12.5 (0.45×0.45)	NA	10	Arlon TC600	6.15	0.508	2 air	NA
[8], single layer cross loop with a square ring slot	599	10.7 × 10.7 (0.51×0.51)	NA	14	RT5880	2.2	0.508	3 air	NA
[9], single layer circular ring	345	15 × 15 (0.83×0.83)	525	10	NA	3.2	1.57	–	0
[13], double layer circular disk	≅ 500	17.65 × 17.65 (0.94×0.94)	88.23	8.5	FR4	4.4	3	1.5 2nd layer	NA
[16], sliced circular fractal	≅ 550	21 × 21 (0.72×0.72)	45	10	NA	2.2	0.1	3 foam	0.004
[17], single layer Koch's double-ring fractal	421.5	15 × 15 (0.54×0.54)	52.9	10	NA	2.2	1	3 foam	0.004
[21], single layer two circular rings	500	15 × 15 (0.51×0.51)	50	10	Laminate	3.4	0.16	6 foam	0.0009
[23], single layer four concentrated circular rings	382	10 × 10 (0.52×0.52)	NA	15	RT5880	2.2	0.762	3 foam	0.0009
[24], single layer rectangular patch and e-shaped structure	500	25 × 25 (0.53×0.53)	NA	5.8	F4B	2.65	2	4 air	0.002
[25], double layer spider-shaped structure	800	8 × 8 (0.52×0.52)	NA	11.725	Taconic RF 35	3.5	0.76	1.52 2nd layer	0.0018
[26], single layer flower shape	360	16 × 16 (0.75×0.75)	≅ 384	12.5	Rogers 4003	3.55	0.508	1 air	0.0027
This work (case 4)	601.3	18.1 × 18.1 (0.64×0.64)	76.37	10	Taconic TLY-5	3.2	0.16	3 foam	0.0009

phase swing beyond 596° was possible due to the formation of the additional resonance frequency. The split circle element analysis reveals that the proposed unit cell element has a sufficient phase variation range, a decent linear reflection phase, a reasonable slope, and a simple design.

References

[1] D.M. Pozar, S. D. Targonski, and H.D. Syrigos, "Design of Millimeter Wave Microstrip Reflectarrays", *IEEE Transactions on Antennas and Propagation*, vol. 45, no. 2, 287–296, 1997 (https://doi.org/10.1109/8.560348).

[2] J. Huang and J.A. Encinar, *Reflectarray Antennas*, Wiley & Sons, USA, 2007 (ISBN: 9780470178768).

[3] P. Nayeri, F. Yang, and A.Z. Elsherbeni, *Reflectarray Antennas: Theory, Designs, and Applications*, Wiley & Sons, USA, 424 p., 2018 (https://doi.org/10.1002/9781118846728).

[4] Y. Li, M.E. Bialkowski, K.H. Sayidmarie, and N.V. Shuley, "81-Element Single-layer Reflectarray with Double-ring Phasing Elements for Wideband Applications", in *IEEE Antennas and Propagation Society International Symposium*, Toronto, Canada, 2010 (https://doi.org/10.1109/APS.2010.5562103).

[5] H. Bodur and S. Cimen, "Reflectarray Antenna Design with Double Cutted Ring Element for X-band Applications", *Microwave and Optical Technology Letters*, vol. 62, no. 10, pp. 3248–3254, 2020 (https://doi.org/10.1002/mop.32436).

[6] L. Zhang *et al.*, "A Single-layer 10-30 GHz Reflectarray Antenna for the Internet of Vehicles", *IEEE Transactions on Vehicular Technology*, vol. 71, no. 2, pp. 1480–1490, 2022 (https://doi.org/10.1109/TVT.2021.3134836).

[7] R.L. Farias, C. Peixeiro, and M.V.T. Heckler, "Single-layer Dual-band Dual-circularly Polarized Reflectarray for Space Communication", *IEEE Transactions on Antennas and Prop.*, vol. 70, no. 7, pp. 5989–5994, 2022 (https://doi.org/10.1109/TAP.2022.3161552).

[8] V. Lingasamy, M.G.N. Alsath, K.T. Selvan, and R. Jyoti, "A Wideband, Single Layer Reflectarray Antenna with Cross Loop and Square Ring Slot Loaded Patch Elements", *International Journal of Microwave and Wireless Technologies*, vol. 11, no. 7, pp. 1–8, 2019 (https://doi.org/10.1017/S1759078719000187).

[9] M.E. Bialkowski and K.H. Sayidmarie, "Phasing Characteristics of a Single Layer Microstrip Reflectarray Employing Various Basic Element Shapes", in *Proc. of 2008 Int. Workshop on Antenna Technology: Small Antennas and Novel Metamaterials*, Chiba, Japan, pp. 79–82, 2008 (https://doi.org/10.1109/IWAT.2008.4511295).

[10] S.A.M. Soliman, A.M. Attiya, and Y.M. Antar, "Low Profile/Single Layer X-Band Circularly Polarized Reflectarray with a Linearly Polarized Feed", *Progress in Electromagnetics Research M*, vol. 113, pp. 87–99, 2022 (https://dx.doi.org/10.2528/PIERM22070106).

[11] C. Zhang *et al.*, "Ka Band Multi-layer Folded Reflectarray using Dual-polarized Slot Antennas as Unit Cells", in *Proc. of European Space Agency Space Antenna Workshop*, Noordwijk, Netherlands, Oct 2012 (https://artes.esa.int/sites/default/files/03_1745_Zhang1.pdf).

[12] R. Florencio *et al.* "Reflectarray Antennas for Dual Polarization and Broadband Telecom Satellite Applications", *IEEE Transactions on Antennas and Propagation*, vol. 63, no. 4, pp. 1234–1246, 2015 (https://doi.org/10.1109/TAP.2015.2391279).

[13] S.A.M. Soliman, E.M. Eldesouki, and A.M. Attiya, "Analysis and Design of an X-Band Reflectarray Antenna for Remote Sensing Satellite System", *Sensors*, vol. 22, no. 3, art. no. 1166, 2022 (https://doi.org/10.3390/s22031166).

[14] J. Huang, and R.J. Pogorzelski, "A Ka-band Microstrip Reflectarray with Elements Having Variable Rotation Angles", *IEEE Transactions on Antennas and Propagation*, vol. 46, no. 5, pp. 650–656, 1998 (https://doi.org/10.1109/8.668907).

[15] R. Florencio *et al.*, "Design of Ku- and Ka-band Flat Dual Circular Polarized Reflectarrays by Combining Variable Rotation Technique and Element Size Variation", *Electronics*, vol. 9, no. 6, art. no. 985, 2020 (https://doi.org/10.3390/electronics9060985).

[16] K.H. Sayidmarie and M.E. Bialkowski, "Fractal Unit Cells of Increased Phasing Range and Low Slopes for Single-layer Microstrip Reflectarrays", *IET Microwaves, Antennas, and Propagation*, vol. 5, no. 11, pp. 1371–1379, 2010 (https://doi.org/10.1049/iet-map.2010.0581).

[17] K.H. Sayidmarie and A.M. Saleh, "Comparison of Phase Responses of Proposed Element Shapes for Reflectarray Unit Cells", in *International Symposium on Microwave, Antenna, Propagation and EMC Technologies for Wireless Communications (MAPE)*, Beijing, China, 2011 (https://doi.org/10.1109/MAPE.2011.6156273).

[18] S. Costanzo *et al.*, "Fractal Reflectarray Antennas: State of Art and New Opportunities", *International Journal of Antennas and Propagation*, art. no. 7165143, 2016 (https://dx.doi.org/10.1155/2016/7165143).

[19] E. Ozturk and B. Saka, "Multilayer Minkowski Reflectarray Antenna with Improved Phase Performance", *IEEE Transactions on Antennas and Propagation*, vol. 69, no. 12, pp. 8961–8966, 2021 (https://doi.org/10.1109/TAP.2021.3090533).

[20] M.H. Dahri *et al.*, "A Novel Asymmetric Patch Reflectarray Antenna with Ground Ring Slots for 5G Communication Systems", *Electronics*, vol. 9, no. 9, art. no. 1450, 2020 (https://doi.org/10.3390/electronics9091450).

[21] M.E. Bialkowski and K.H. Sayidmarie, "Investigations into Phase Characteristics of a Single-layer Reflectarray Employing Patch or Ring Elements of Variable Size", *IEEE Transactions on Antennas and Propagation*, vol. 56, no. 11, pp. 3366–3372, 2008 (https://doi.org/10.1109/TAP.2008.2005470).

[22] K.H. Sayidmarie and A.M. Saleh, "Evaluation of Phase Responses of Double Ring Elements for Reflectarray by Simulation and Measurement", in *Fourth International Conference on Computational Intelligence, Communication Systems and Networks*, Phuket, Thailand, 2012 (https://doi.org/10.1109/CICSyN.2012.30).

[23] L. Veluchamy, K.T. Selvan, R. Jyoti, and S.S. Kumar, "Wideband Reflectarray Antennas using Concentric Ring-based Elements for Ku-band Applications", *IETE Journal of Research*, vol. 69, no. 3, pp. 1675–1685, 2023 (https://doi.org/10.1080/03772063.2021.1874842).

[24] H. Zhang *et al.*, "A Single-layer Circularly Polarized Reflectarray Antenna with High Aperture Efficiency for Microwave Power Transmission", *International Journal of Antennas and Propagation*, art. no. 1569710, 2023 (https://doi.org/10.1155/2023/1569710).

[25] M. Elahi, T. Jeong, Y. Yang, K.-Y. Lee, and K.C. Hwang, "A Wideband Reflectarray Antenna for Satellite Application with Low Cross-polarization", *Applied Science*, vol.13, no. 7, art. no. 4545, 2023 (https://doi.org/10.3390/app13074545).

[26] E. Hadian, M-M. Askhiri, S. Fakhte, and D.Ramezani, "Design of a Wideband Flower-like Shape Metamaterial Reflectarray Antenna", *IETE Journal of Research*, 2023 (https://doi.org/10.1080/03772063.2023.2173671).

Khalil H. Sayidmarie, Professor
College of Electronics Engineering
https://orcid.org/0000-0001-6525-0949
E-mail: kh.sayidmarie@uoninevah.edu.iq
Ninevah University, Mosul, Iraq
https://uoninevah.edu.iq

Likaa S. Yahya, Ph.D.
Institute of Technology
https://orcid.org/0000-0003-2965-158X
Northern Technical University, Mosul, Iraq
https://ntu.edu.iq